09,03

Excitation of terahertz radiation in $p-n$-heterostructures based on a-Si : H/c-Si

© *A.V. Andrianov*[1], *A.N. Aleshin*[1], *S.N. Abolmasov*[1,3], *E.I. Terukov*[1,2,3], *A.O. Zakhar'in*[1]

[1] Ioffe Institute,
St. Petersburg, Russia
[2] St. Petersburg State Electrotechnical University „LETI",
St. Petersburg, Russia
[3] R & D Center of Thin Film Technologies in Energetics LLC,
St. Petersburg, Russia

E-mail: alex.andrianov@mail.ioffe.ru

Studies on the generation of terahertz (THz) radiation in $p-n$-heterostructures based on a-Si : H/c-Si upon their photoexcitation by a femtosecond titanium-sapphire laser with a wavelength of 800 nm are presented. The properties of observed THz radiation allow to explain its nature by excitation of fast photocurrent of nonequilibrium charge carriers created in the region of the potential barrier under femtosecond interband photoexcitation of the structure. The fast photocurrent, in turn, emits THz electromagnetic waves. The waveforms and amplitude spectra of the observed THz radiation reflect the dynamics of photoexcited charge carriers in the structures. The intensity of THz radiation observed in the studied $p-n$-heterostructures based on a-Si : H/c-Si is comparable to that generated in n-InAs crystals, which are widely used as emitters in systems of THz time-domain spectroscopy. Therefore, a-Si : H/c-Si $p-n$-heterostructures can be used as THz emitters for need of THz spectroscopy.

Keywords: femtosecond laser photoexcitation, heterostructures, fast photocurrent, terahertz electromagnetic radiation.

1. Introduction

Generation of electromagnetic waves in terahertz (THz) range (from 0.1 to 10 THz) using ultra-short, pilsed, visible or near infrared (NIR) lasers is currently widely used in THz time domain spectroscopy (THz-TDS) and THz visualization of various objects [1–3]. The benefit of THz-TDS devices is that all main device components (both THz radiation source and receiver) are operated at room temperature and in such devices the signal-to-noise ratio of the signal amplitude may reach 10^4 or even higher (and not less than 10^8 for power) [4].

Generation of THz radiation pulses containing several electromagnetic oscillation cycles was observed when various semiconductors and semiconductor structures were exposed to femtosecond laser excitation. In general, such THz generation mechanism is due to fast dipole or short photocurrent burst excitation in the material or the structure [5,6]. In the far field, the amplitude of the THz wave generated in such way E_{THz}, is proportional to $\frac{\partial^2 P}{\partial t^2}$ or $\frac{\partial J}{\partial t}$, where $P(t)$ and $J(t)$ are the tine-varying dipole moment and photocurrent induced by femtosecond laser radiation, respectively.

Among THz emitters based on semiconductors, emitters using photoconducting bias antennas [7], and THz-„surface" emitters based on semiconductor surface excitation are the most widely used. In the latter case, two mechanisms of the THz radiation generation are possible: fast photocurrent burst of non-equilibrium carriers in the near-surface electric field and Dember photocurrent (or Dember dipole) directed into the crystal volume and caused by the diffusion coefficient difference for electrons and holes. Dember effect is the main mechanism of THz generation in „surface" emitters based on InAs crystals [8], which are today the most simple and efficient THz radiation sources.

Bulk silicon is considered to be rather unsuitable as a „surface" THz emitter [9] primarily due to low absorption of femtosecond pumping laser radiation in the material and, therefore, due to large thickness of the non-equilibrium charge carrier generation region in comparison with the surface electric field localization region. However, authors in Ref. [10] showed that Si $p-i-n$-photodiode can serve as high performance THz emitter when it is exposed to photoexcitation with ultra-short laser pulses due to fast photocurrent generation in the structure. High performance of such emitter can be provided in the case when light absorption depth is comparable or less than the size of i-region where the electric field is concentrated.

In this work studies of THz radiation generation in $p-n$-heterostructures based on a-Si : H/c-Si caused by femtosecond pulsed laser photoexcitation at 800 nm are discussed.

2. Experiment details

The studied structures are crystalline silicon solar cells (c-Si SC) manufactured using heterojunction technology (HJT) [11,12], that capture a significant portion of solar radiation spectrum and have rather high energy conversion efficiency. The insert in Fig. 1, a shows the cross-sectional view of the device structure. Heterostructures were formed on n-type silicon substrate with a resistivity $1.5\,\mathrm{Ohm \cdot cm}$ and a thickness of about $140\,\mu m$, textured on both sides by chemical etching in order to increase light absorption and minimize its reflection from the SC surface [11]. ITO (indium tin oxide that is transparent in visible and NIR ranges) contact layer thicknesses were $100\,\mathrm{nm}$. (p) a-Si:H layer at the front surface of SC was $15\,\mathrm{nm}$ in thickness and was boron-doped up to $10^{19}\,\mathrm{cm}^{-3}$. Both front and rear ($i$) a-Si:H layers had a thickness of approximately $5\,\mathrm{nm}$. The rear (n) a-Si:H layer was about $15\,\mathrm{nm}$ thick and was phosphorus-doped up to $10^{21}\,\mathrm{cm}^{-3}$. Metal (silver) strips with a thickness about $40\,\mu m$ were screen printed on the surface of front and rear ITO layers to collect effectively the current in the SC. The metal strip spacing was $1\,\mathrm{mm}$ and $1.5\,\mathrm{mm}$ on the front and rear surface of the device.

The insert in Fig. 1, a shows the THz experiment geometry. The test structured were excited by femtosecond titanium-sapphire laser with a wavelength of $800\,\mathrm{nm}$ and a pulse duration of $15\,\mathrm{fs}$ at repetition frequency $80\,\mathrm{MHz}$. Laser radiation with p-polarization was focused into a spot with size about $250\,\mu m$ between metal strips. The maximum excitation pulse energy was equal to $5\,\mathrm{nJ}$. Laser radiation was emitted onto the structure at an angle close to 45 degrees. THz radiation generated in the structure was collected in the direction of mirror reflection from the front surface of the structure using parabolic reflective optics and was delivered to a THz detector. Detection was carried out by electrooptical THz waveform sampling in $1\,\mathrm{mm}$ (110) ZnTe crystal (for details of the experimental setup, see [13]).

3. Results and discussion

It was found that at zero bias voltage applied to the studied structure, the THz radiation signal is very weak and its amplitude is comparable with noise (signal-to-noise ratio max. $1.5−2$), and there is no signal in the case of small forward bias. The THz radiation signal occurs when a reverse bias is applied and its amplitude grows considerably with bias voltage growth. Thus, at $−9\,\mathrm{V}$, the THz radiation signal is approximately 70 times higher in comparison with the signal at $0\,\mathrm{V}$. Figure 1, a shows typical THz radiation waveform (electric field time sweep of THz wave) at bias voltage $−9\,\mathrm{V}$, and Figure 1, b shows THz radiation amplitude spectrum. The THz radiation spectrum extends up to $2.2\,\mathrm{THz}$ (such upper frequency limit corresponds to 0.01 from the maximum). The observed THz waveform and amplitude spectrum shape are affected by absorption in water vapors (measurements were carried out
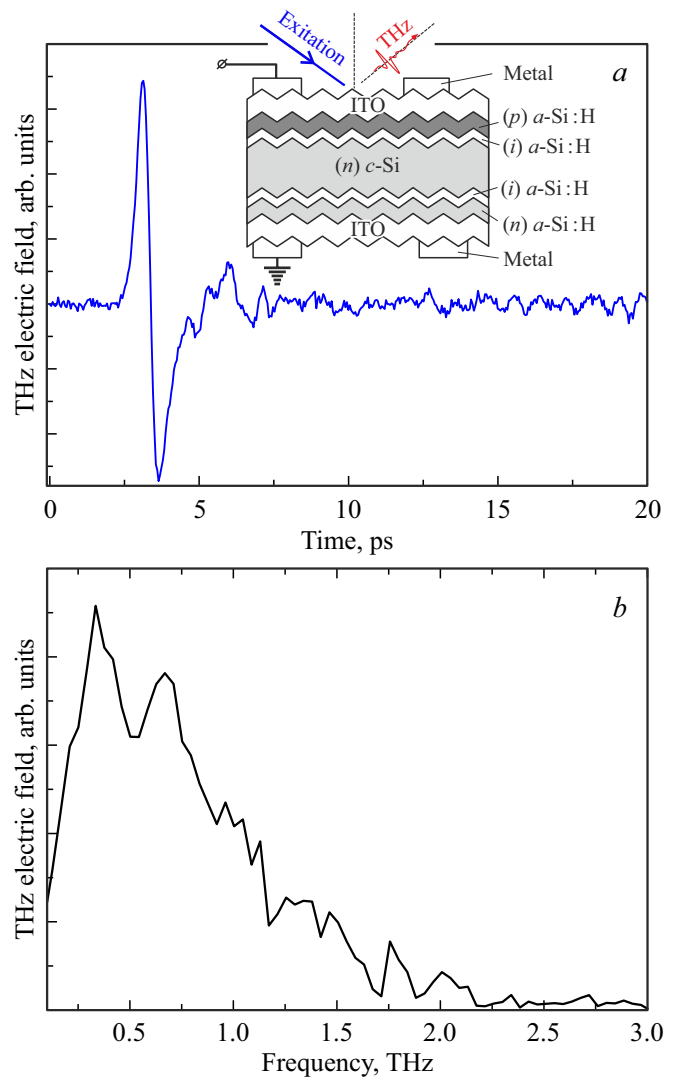
Figure 1. a) Typical THz radiation waveform generated in the $p−n$-heterostructure based on a-Si : H/c-Si. Reverse-bias voltage is $9\,\mathrm{V}$, average pumping radiation power is $117\,\mathrm{mW}$. The insert schematically shows the design of the studied structure and THz experiment geometry. b) The THz radiation amplitude spectrum obtained by THz waveform Fourier transformation as shown in Figure 1, a.

in ambient air) and due to low reflections of THz radiation from the internal layers of the device.

The $800\,\mathrm{nm}$ femtosecond pumping laser radiation passes through a-Si:H layers almost without absorption and is completely absorbed within c-Si where the main electric field of $p−n$-junction is also concentrated. Hence non-equilibrium carriers created by pumping are accelerated in this field and lead to the photocurrent burst resulting in generation of the observed THz radiation. In addition, the front ITO layer, which thickness ($100\,\mathrm{nm}$) is significantly less than the radiation wavelength and the skin layer thickness is transparent to THz radiation [14]. Therefore, THz radiation generated at $p−n$-junction in the studied
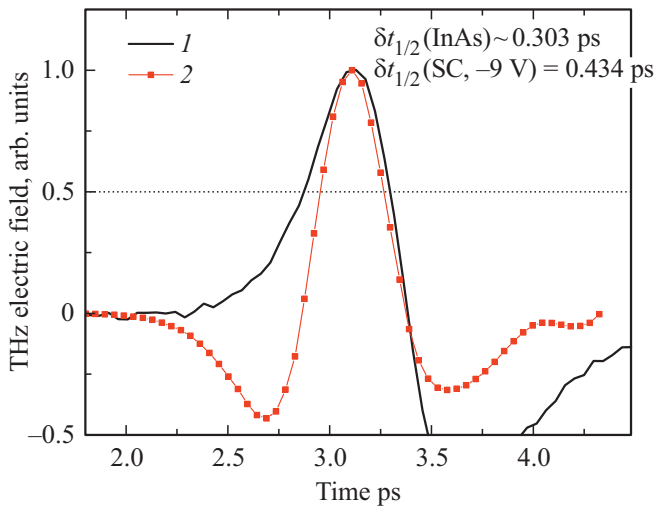
Figure 2. THz waveforms generated in the $p-n$-heterostructure based on a-Si : H/c-Si at a reverse bias voltage of 9 V (*1*) and in n-InAs (*2*) crystal exposed by pulsed titanium-sapphire laser with average laser power about 117 mW (15 fs pulse duration, 800 nm). Signals are normalized to the maximum. In both cases, THz radiation was detected by electrooptical THz waveform sampling in a 1 mm (110) ZnTe plate.

structure is observed in the reflection geometry (Figure 1, a, Insert)

The fact that THz generation signal in the studied structures is almost absent at zero bias, but appears at reverse bias across the structure and grows significantly with reverse bias voltage growth, could suggest that electric-field-induced optical rectification (EFIOR) contributes to THz generation [15,16]. It is known that the optical rectification effect and, in particular, EFIOR leads to generation of fast dipole moment that initiates THz radiation when the material is exposed to ultrashort laser pulses [1–3]. It

should be mentioned that nonlinear optical effects, including the optical rectification effect, are almost inertialess at time scale in the region of the pumping laser pulse duration (15 fs in our case). Figure 2 shows a comparison between maximum-normalized THz waveforms generated in n-InAs crystal (standard emitter in the THz-TDS-test setup [4,13]), and in the studied $p-n$-heterostructure based on a-Si : H/c-Si with photoexcitation and detection in similar conditions. It can be seen that half width (full width at half maximum) of the positive THz pulse burst from the studied structure is about 434 fs, and half width of the positive THz pulse burst from n-InAs is about 303 fs. In other words, there is time delay about 130 fs in the THz pulse generated in the studied structure compared with THz pulse from n-IaAs crystal. This suggests that THz generation in $p-n$-heterostructures based on a-Si : H/c-Si is more inertial than in n-InAs crystal where, as mentioned above, THz generation was primarily caused by Dember effect. Therefore, THz radiation observed in $p-n$-heterostructures based on a-Si : H/c-Si is not associated with the EFIOR effect, and is caused by formation of fast photocurrent of non-equilibrium electrons and holes in the structure exposed to femtosecond interband photoexcitation.

Figure 3, a shows the dependence of the THz pulse amplitude on the reverse bias voltage in the structure. The shape of this curve can be explained by the growth of the region where the electric field of $p-n$-junction is concentrated and by the growth of the non-equilibrium charge carrier rate in this field when the reverse bias voltage increases. Interestingly, at -30 V across the studied structure, the THz signal amplitude is only 3 times less than in the case when n-InAs crystal is used a THz emitter, which is the main source of THz emission in the THz-TDS-device used in the experiment in Ref. [4,13]. Therefore, we can conclude that THz emitters based on a-Si : H/c-Si $p-n$-heterostructures may be used for THz spectroscopy purposes as well.
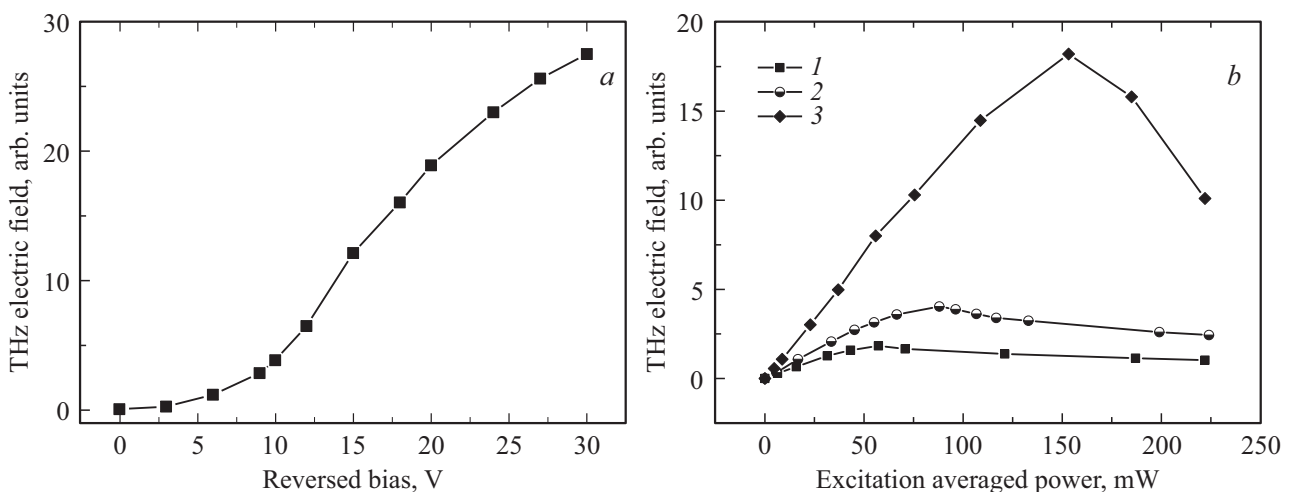
Figure 3. a) Dependence of the THz pulse amplitude generated in the $p-n$-heterostructure based on a-Si : H/c-S on the reverse bias voltage at an average pumping laser power of 153 mW. b) Dependence of the THz pulse amplitude on the average pumping laser power at various reverse bias voltages. *1* — 6, *2* — 9, *3* — 20 V.
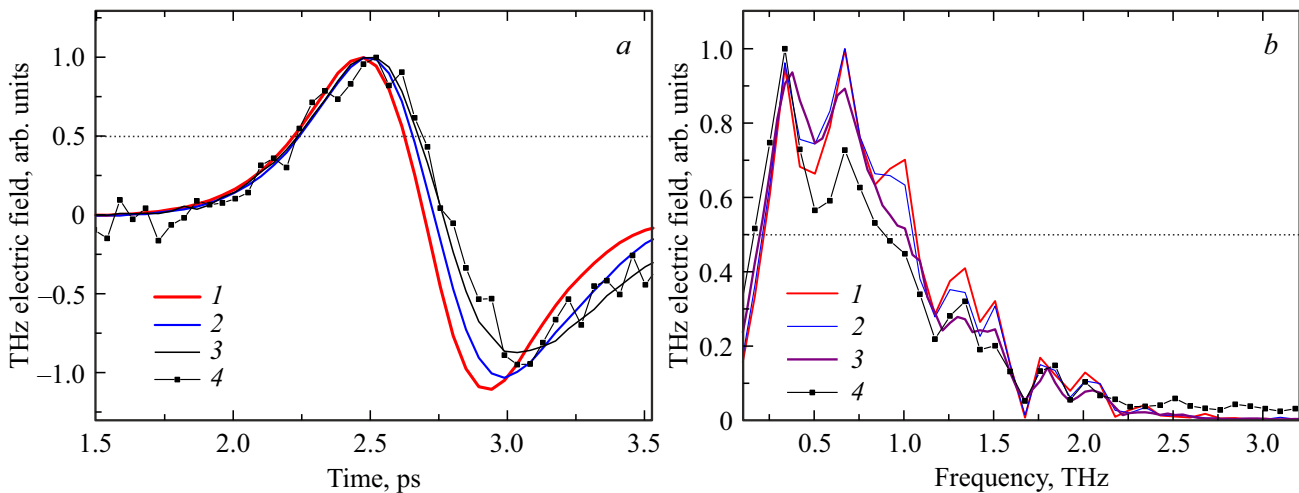
Figure 4. *a*) Normalized to maximum waveforms of the THz radiation generated in the $p-n$-heterostructure based on a-Si : H/c-Si at various reverse bias voltages (*1−4*). *b*) Normalized to maximum THz radiation amplitude spectra at various reverse bias voltages (*1−4*). Average pumping laser power was equal to 153 mW. *1* — 30, *2* — 20, *3* — 10, *4* — 3 V.

Figure 3,*b* shows the dependence of pulse amplitude of the generated THz radiation on the average pumping laser power. It can be seen that the dependence is nonmonotonic with a maximum followed by THz amplitude decay. Such dependence of the THz pulse amplitude on the photoexcitation power may be explained by the effect of electric field screening in $p-n$-heterostructures by non-equilibrium carriers at high photoexcitation level. The fact that the optimum pumping laser power, i.e. the power corresponding to the THz signal maximum, increases with reverse bias growth also supports this explanation. It should be noted that the effect of electric field screening by non-equilibrium charge carriers in $p-n$-junctions based on InGaAs and the influence of this effect on the THz radiation generation when such structures are exposed to femtosecond laser photoexcitation were observed earlier, see, for example Ref. [17].

Figure 4,*a* shows normalized to maximum THz waveforms measured at various reverse bias voltages. It can be seen that the THz pulse narrows with growth of bias voltage. During transition from −3 to −30 V, half width (pulse width at 0.5 from the maximum value) of THz pulse is reduced by about 70 fs. Also in this case, the THz pulse maximum position is shifted to earlier time moments with bias voltage growth. Figure 4,*b* illustrates THz radiation amplitude spectra at various bias voltages. It can be seen that the THz radiation spectrum expands considerably with bias voltage growth. Both THz waveforms and amplitude spectra reflect the behavior of non-equilibrium electrons and holes generated by femtosecond laser pumping in the electric field of $p-n$-heterostructure. With the growth of bias voltage and, therefore, with electric field growth, photocurrentgrowth rate of non-equilibrium carriers created by the femtosecond laser pulse increases, which, in turn, results in narrowing of the generated THz pulse and expansion of its spectrum.

4. Conclusion

Generation of THz radiation in $p-n$-heterostructures based on a-Si : H/c-Si (c-Si SC manufactured by using HJT technology) caused by photoexcitation of femtosecond titanium-sapphire laser at 800 nm has been investigated. THz radiation is observed at reverse bias voltages across the c-Si SC and its intensity grows significantly with bias voltage growth. Properties of the observed THz radiation allow to associated it with the excitation of fast photocurrent of non-equilibrium charge carriers produced by femtosecond interband photoexcitation at the potential barrier in the device. The fast photocurrent, in turn, emits a THz wave. Nonmonotonous dependence of the THz pulse amplitude on the laser photoexcitation intensity was detected and explained by the effect of electric field screening in the $p-n$-heterostructure by non-equilibrium carriers at high photoexcitation level. Waveforms and amplitude spectra of the observed THz radiation reflect the behavior of photoexcited charge carriers is the heterostructures. With optimum intensity of the interband laser photoexcitation, the THz radiation pulse amplitude observed in the studied $p-n$-heterostructures based on a-Si : H/c-Si is comparable with THz radiation generated in n-InAs crystals that are widely used as emitters in THz-TDS devices. Therefore, a-Si : H/c-Si $p-n$-heterostructure may be used as THz emitters for THz spectroscopy purposes. Moreover, further investigations of THz generation processes may provide new opportunities for detailed study of non-equilibrium carrier behavior at subpicosecond time scale in HJT-solar cells.

Conflict of interest

The authors declare that they have no conflict of interest.

References

[1] Yun-Shik Lee. Principles of Terahertz Science and Technology. Springer Science + Business Media, LLC (2009). 340 p.

[2] J. Neu, C.A. Schmuttenmaer. J. Appl. Phys. **124**, 231101 (2018).

[3] Terahertz Spectroscopy and Imaging / Eds K.-E. Peiponen, J.A. Zeitler, M. Kuwata-Gonokami. Springer-Verlag, Berlin, Heidelberg (2013). 641 p.

[4] A.V. Andrianov, A.N. Aleshin, L.B. Matyushkin. Pis'ma v ZhETF **109**, 30 (2019). (in Russian).

[5] Terahertz Optoelectronics / Ed. K. Sakai. Springer-Verlag, Berlin (2005). 387 p.

[6] V.L. Malevich, P.A. Ziaziukia, R. Norkus, V. Pacebutas, I. Nevinskas, A. Krotkus. Sensors **21**, 4067 (2021).

[7] A.E. Yachmenev, D.V. Lavrukhin, I.A. Glinsky, N.V. Zenchenko, Y.G. Goncharov, I.E. Spektor, R.A. Khabibullin, T. Otsuki, D.S. Ponomarev. Opt. Eng. **59**, 061608 (2019).

[8] C. Song, P. Wang, Y. Qian, G. Zhou, R. Notzel. Opt. Express **28**, 25751 (2020).

[9] G. Ramakrishnan, G.K.P. Ramanandan, A.J.L. Adam, M. Xu, N. Rumar, R.W.A. Hendrikx, P.C.M. Planken. Opt. Express **21**, 16784 (2013).

[10] L. Xu, X.-C. Zhang, D.H. Auston, B. Jalali. Appl. Phys. Lett. **59**, 3357 (1991).

[11] E. Terukov, A. Kosarev, A. Abramov, E. Malchukova. From 11% Thin Film to 23% Heterojunction Technology (HJT) PV Cell: Research, Development and Implementation Related $1600 \times 1000\,mm^2$ PV Modulesin Industrial Production. IntechOpen, Solar Panels and Photovoltaic Materials (2018). Ch. 5.

[12] A.S. Abramov, D.A. Andronikov, S.N. Abolmasov, E.I. Terukov. Silicon Heterojunction Technology: A Key to High Efficiency Solar Cells at Low Cost. In: High-Efficient Low-Cost Photovoltaics / Eds V. Petrova-Koch, R. Hezel, A. Goetzberger. Springer Nature Switzerland AG (2020). Ch. 7. P. 113−132.

[13] A.V. Andrianov, A.N. Aleshin, V.N. Truhin, A.V. Bobylev. J. Phys. D **44**, 265101 (2011).

[14] A.V. Andrianov, A.N. Aleshin, S.N. Abolmasov, E.I. Terukov, E.V. Beregulin. Pis'ma v ZhETF **116** (825), (2022). (in Russian).

[15] J.F. Ward, J.K. Guha. Appl. Phys. Lett. **30**, 276 (1977).

[16] S.L. Chuang, S. Smitt-Rink, B.I. Greene, P.N. Saeta, A.F.J. Levi. Phys. Rev. Lett. **68**, 102 (1992).

[17] Y. Kadoya, T. Matsui, A. Takazato, J. Kitagawa. Joint Proc. of 32nd Int. Conf. Infrared and Millimeter Waves and the 15th Int. Conf. on Terahertz Electronics (02−09 September 2007) Cardiff, UK. P. 987−988.

Translated by E.Ilyinskaya